Steady-State Kinetic Studies of Dithionite Utilization, Component Protein Interaction, and the Formation of an Oxidized Iron Protein Intermediate during *Azotobacter vinelandii* Nitrogenase Catalysis†

J. L. Johnson,‡ A. M. Tolley,‡ J. A. Erickson, and G. D. Watt*

Department of Chemistry and Biochemistry, Brigham Young University, Provo, Utah 84602

Received October 30, 1995; Revised Manuscript Received June 17, 1996⊗

ABSTRACT: Steady-state kinetic analysis of the two-component protein system of *Azotobacter vinelandii* (Av) nitrogenase is reported. A precisely obeyed half-order reaction in dithionite was observed at concentrations up to 21 mM with no indication of saturation by this substrate. This behavior was monitored by optical, amperometric, and manometric kinetic techniques, and the results were mathematically fit to establish the half-order reaction in dithionite. Under conditions where the MgATP and dithionite concentrations remain unchanged, Av2 (the Fe protein component) interacts with Av1 (the MoFe protein component according to the rate law, suggesting a rapid 1:1 Av2−Av1 interaction:

$$v = \frac{\mathrm{d}[H_2]}{\mathrm{d}t} = \frac{k_{cat}[\mathrm{Av1}][\mathrm{Av2}]}{K + [\mathrm{Av2}]} = \frac{V_{max}[\mathrm{Av2}]}{K + [\mathrm{Av2}]}$$

with [Av2] the free Fe protein concentration, $K = 5.9\ \mu$M, and $V_{max} = 2134$ nmol of H_2 min^{-1} (mg of Av1)$^{-1}$. Under dithionite-depleted conditions, Av2 undergoes an Av1-mediated, one-electron oxidation, consistent with its proposed role as a specific, single-electron reductant for Av1. During steady-state turnover as a function of Av2/Av1 ratio, optical spectroscopy demonstrated the presence of 25−30% oxidized Av2 as an enzyme intermediate. Computer-averaged EPR spectra showed that Av1 was >95% EPR-silent and Av2 was up to 30% oxidized (Av2ox), consistent with the optical measurements. These optical and EPR results show that up to six Av2ox per Av1 can accumulate in the presence of dithionite during catalysis, suggesting that the conversion of Av2ox back into Av2red is a relatively slow process.

In all biological systems thus far examined, nitrogenase activity ($N_2 + 8H^+ + 8e^- = 2NH_3 + H_2$) results from the interaction of two dissimilar, multisubunit, metalloproteins (the MoFe protein, $\alpha_2\beta_2$, MW = 230 000; and the Fe protein, α_2, MW = 63 000) and requires a source of low-potential electrons, MgATP, and small reducible molecules (N_2, H^+, acetylene, etc.) as substrate (Mortenson & Thorneley, 1979; Orme-Johnson, 1985; Smith & Eady, 1992; Kim & Rees, 1994).

Steady-state (Silverstein & Bulen, 1970; Watt, 1977; Watt & Burns, 1977; Hageman & Burris, 1978) and pre-steady-state (Hageman et al., 1980) kinetic studies have been reported for *Azotobacter vinelandii* (Av) nitrogenase and its component proteins in order to discern the sequence of substrate addition, to elucidate and describe enzyme intermediates, to evaluate the role of protein−protein interactions, and to determine other important steps occurring during nitrogenase catalysis. However, because of the inherent complexity of this system and technical complications such as its O_2 sensitivity, there remain gaps in our understanding of nitrogenase catalysis and disagreements in some of the reported results. For example, Watt (1977) and Watt and Burns (1977) initially reported amperometric steady-state kinetic measurements of Av nitrogenase catalysis from which an overall rate law was derived, both confirming the second-order dependence on MgATP (Bulen & Silverstein, 1970) and demonstrating a half-order, nonsaturating rate dependence on dithionite (Watt et al., 1975), first observed from calorimetric measurements (Watt and Bulen, 1974).

Hageman and Burris (1978) reexamined the dithionite dependence during nitrogenase catalysis by optical kinetic methods, and from their slope analysis of progress curves they reported that enzyme saturation with dithionite occurred at concentrations above 14 mM. The zero-order reaction observed by Hageman and Burris (1978) differs from the half-order reaction reported by Watt and Burns (1977), and this disagreement presents a problem of interpretating how low-potential electrons are processed by the Av nitrogenase component proteins during nitrogenase catalysis. Resolution of this kinetic disagreement is important for a proper understanding of how electrons enter into the nitrogenase catalytic cycle.

Another feature of nitrogenase catalysis that was recognized early but has received little study since then is the enzyme intermediates of both the MoFe and Fe proteins first observed during catalysis by EPR measurements for Av (Orme-Johnson et al., 1972), *Clostridium pasteuranium,* (Cp ((Mortenson et al., 1973), and *Klebsiella pneumonia* (Kp) (Smith et al., 1973) nitrogenase proteins. Under turnover conditions, the MoFe protein was observed to be nearly EPR-silent (and presumed further reduced than the resting state) and the Fe protein was found to be partially EPR-silent (and

† This research was supported by Grant 82-CRCR-1-1122 from the USDA/SEA Competitive Grants Program to G.D.W.

* To whom correspondence should be addressed.

‡ Brigham Young University Undergraduate Research Program.

⊗ Abstract published in *Advance ACS Abstracts,* August 1, 1996.

S0006-2960(95)02581-5 CCC: $12.00

presumed partially oxidized). Further identification, characterization, and quantitation of these intermediates and a detailed examination of their formation by steady-state kinetic methods should assist in interpreting the overall kinetic behavior of the component proteins during catalysis.

Here we report detailed steady-state kinetic measurements of the dithionite reaction with the nitrogenase proteins, resolving the uncertainty in the reaction order of this reductant, by showing it conforms to a half-order reaction as expected for $S_2O_4^{2-} = 2SO_2^{-\bullet}$, with $SO_2^{-\bullet}$ being the actual nitrogenase reductant. We also report optical spectroscopic measurements of the oxidized Fe protein (Av2ox) intermediate that occurs during steady-state turnover. These latter measurements provide a basis not only for identifying and quantitating this intermediate but also for gaining information regarding the conditions of its formation. The applicability of the Thorneley−Lowe scheme (Thorneley & Lowe, 1983, 1984a,b, 1985) to the steady-state formation of this Av2ox intermediate is also considered.

MATERIALS AND METHODS

Nitrogenase component proteins were prepared from *Azotobacter vinelandii* cells by the procedure of Burgess et al. (1980). The Sussex designation (Thorneley & Eady, 1973) is used for the MoFe protein (Av1) and Fe protein (Av2) from *Azotobacter vinelandii*, and Av2/Av1 values refer to molar ratios. Dithionite utilization during hydrogen evolution (Wherland et al., 1981; Bulen et al., 1965) using Millipore-filtered solutions was used to assess nitrogenase activity. Sodium dithionite ($Na_2S_2O_4$) was recrystallized repeatedly (Noguchi, 1971; McKenna, 1991) and dried under vacuum at 70 °C to attain $Na_2S_2O_4$ of >98% purity. The solid $Na_2S_2O_4$ was stored at −20 °C under N_2 or in a vacuum atmospheres glovebox until used. ATP, creatine phosphokinase, Tris buffer, and creatine phosphate were obtained from Sigma.

Steady-State Nitrogenase Reactions. Three different kinetic procedures were used to examine and evaluate various aspects of Av nitrogenase kinetics under steady-state conditions. All three procedures utilized the ATP generating system containing creatine phosphokinase at 15 mM to maintain a constant ATP concentration of 5 mM for at least 30 min under the conditions used.

(a) H_2 Evolution. The rate (or amount) of H_2 evolved from 1.0 mL assays containing the MgATP generating system (5 mM ATP), initial dithionite concentrations of 10−40 mM, and selected molar ratios of Av2/Av1 (0.4−50) was followed by manometric methods (Bulen et al., 1965) for continuous assays or by gas chromatography (Wherland et al., 1981) for fixed time (10 min) quenched assays.

(b) Optical Spectroscopy. The rate of dithionite depletion as a function of dithionite concentration up to 21 mM was measured using a Cary 118 spectrophotometer at 350 nm (ϵ = 1300 cm^{-1} M^{-1}), 370 nm (ϵ = 116 cm^{-1} M^{-1}), or 375 nm (ϵ = 71 cm^{-1} M^{-1}) in 1 cm anaerobic, thermostated quartz cells, following the procedure of Hageman and Burris (1978). Spontaneous dithionite decomposition in the absence of nitrogenase proteins monitored at these wavelengths over 30 min was negligible compared to the enzyme-catalyzed reactions. The dithionite absorbance was amplified 10−20 times (run on 0.1−0.2 absorbance range) and electronically offset to be on scale. The decrease in dithionite concentration under these high sensitivity conditions was recorded at one of the indicated wavelengths as a function of time. The spectrophotometer output was scanned by a Hewlet Packard Scan Jet Plus and digitized using Un-Scanit Software to obtain 600−2000 individual points (typically, one or two points per second). The reactions were followed 15−30 min to collect a detailed data set, during which time the optical cell was removed periodically to check for and remove any H_2 bubbles forming in the optical path. The presence of bubbles or particles from unfiltered solutions can significantly alter the dithionite absorbance changes being measured under these high-resolution, low light transmission conditions. The absorbance vs time data files were imported into an Excel spread sheet or an Applied Photophysics Kinetics Global Analysis Program where the data were mathematically fit to determine the reaction order and to precisely evaluate the rate law for enzymatic dithionite utilization.

(c) Amperometric Method. The same amperometric method and procedures previously described for monitoring dithionite disappearance (Watt & Burns, 1977) were used except that dithionite concentrations up to 20 mM were examined. The reaction was initiated by adding Av2 to a reaction mixture containing Av1, the ATP generating system, and various levels of dithionite (5−20 mM). The change in anodic diffusion current over 10−30 min reaction times (producing 100−500 data points) was used to evaluate the rate law for dithionite utilization using the computer-fitting procedures described above.

Steady-State Levels of Av2ox. Optical spectroscopy was used to measure the steady-state level of Av2ox during nitrogenase turnover. ATP generating solution (pH 7.5), without ATP, dithionite at 5−20 mM, and various ratios of Av2/Av1 (1−40) at constant Av1 were placed in a 1.0 mL anaerobic optical cell, and the spectrum for reduced Av1 and Av2 was recorded between 800 and ∼380 nm (dithionite absorption limits the lower wavelength value). The reaction was initiated by adding ATP to a final concentration of 5 mM, and the spectrum was recorded after steady state was attained (1−3 min). A final spectrum was recorded when all dithionite was utilized.

The steady-state level of Av2red was also measured for Av2/Av1 ratios of 12.0, 18.2, and 24.1 by EPR spectroscopy in calibrated 3 mm EPR tubes at g = 1.94 using the conditions and procedures outlined for the optical measurements above and previously reported EPR results (Orme-Johnson et al., 1972; Smith et al., 1973; Mortenson et al., 1973). The integrated intensities for the g = 2 region of 4−16 computer-averaged spectra obtained at 13 K for steady-state samples were compared to appropriate controls to quantitatively determine the decrease in the Av2red concentration at steady state. Two separate EPR controls were prepared: (1) an EPR sample containing all reaction components except Av1 (no turnover occurs, but Av2 is fully reduced and in its MgATP-bound form); and (2) Av1 and Av2 both in the presence of 20 mM dithionite but in the absence of MgATP. EPR control 1 was compared directly to the steady-state sample with identical Av2 concentration because Av2 was present in the nucleotide-bound form in both cases. Also, this control had no interference with the sharp g = 2.01 signal from Av1 which was absent during turnover. With control 2, direct comparison to the steady-state spectrum for identical Av2 samples could not be made because Av2 was in the nucleotide form during steady state but not in the control. In this case, a correction for the difference in intensity between ATP-bound (0.26 spin/Av2)

Table 1: Av1 Activity as a Function of Av2/Av1 Ratio and $S_2O_4^{2-}$ Concentration

	$[S_2O_4^{2-}]$ (mM)				
Av2/Av1[a]	5	10	20	30	40
5	744	818	818	609	414
10	1280	1350	1398	1184	1013
20	1450	1590	1680	1510	1270

[a] The specific activity in nanomoles of H_2 per minute per milligram of Av1 of various Av2/Av1 ratios as a function of initial $S_2O_4^{2-}$ concentrations using fixed time (10 min) quenched assays.

and ATP-free (0.21 spin/Av2) was made. This correction agreed with previously published (Watt & McDonald, 1985) Av2 spin intensity measurements in the ATP-bound and ATP-free states. The $g = 2.01$ signal from Av1 was present, but because relatively large Av2/Av1 ratios were used (12, 18.1, and 24.2), the error from this source was small. Corrections using both type 1 and 2 controls were made to the steady-state samples and found to be nearly identical. For example, at a 12:1 Av2/Av1 ratio (see Figure 4), the steady-state sample gave 10 587 integrated units compared to 16 287 (control 1) and 16 155 (control 2) corrected integrated units for the Av2 controls. These results show a 65% decrease in Av2red concentration at steady state compared to the control, yielding a distribution of 7.8 Av2red and 4.2 Av2ox in the steady state. This same procedure was applied for ratios of 18.1 and 24.2 (see Figure 4).

In addition to the EPR integration procedure discussed above, previously published (Orme-Johnson et al., 1972; Smith et al., 1973; Mortenson et al., 1973) EPR results were also analyzed to estimate the decrease in EPR intensity at steady state. In analyzing these previously published results, the signal height of the Fe protein component at steady state was compared to the appropriate signal height of the Fe protein (corrected if necessary) presented under the same conditions. As shown in Figure 4, the results obtained by EPR signal integration as reported here are comparable to results obtained using EPR signal heights.

RESULTS

Rate Dependence on Initial Dithionite Concentration. Table 1 shows the variation of Av1 activity as a function of initial dithionite concentration at Av2/Av1 ratios of 5, 10, and 20. Two effects are seen: (1) optimal Av1 activity occurs near 20 mM for all three ratios and declines above this value, likely due to salt inhibition (Burns et al., 1985; Deits & Howard, 1990); and (2) the apparent salt effect is more pronounced at lower ratios. The kinetic results reported below were obtained near 20 mM $S_2O_4^{2-}$ or below in order to maximize the kinetic effect being monitored and to avoid complications due to apparent salt inhibition by $S_2O_4^{2-}$.

Having established that 20 mM $S_2O_4^{2-}$ provides near-optimum conditions for Av1 activity, the rate dependence was determined for enzymatic production of H_2 as a function of $S_2O_4^{2-}$ concentration. Figure 1 is the initial section of an optical kinetic curve at high sensitivity (Av2/Av1 = 3.7) following the decrease of $[S_2O_4^{2-}]$ during the H_2-evolution reaction. The rate profile is nonlinear at 21 mM, thereby excluding a zero-order reaction in $S_2O_4^{2-}$ and clearly demonstrating that $S_2O_4^{2-}$ is *not* saturating the Av2−Av1 system under optimal rate conditions. Over 1000 points obtained by digitizing Figure 1 were fit to zero-, half-, and first-order rate functions. Zero order (a straight line fit) was

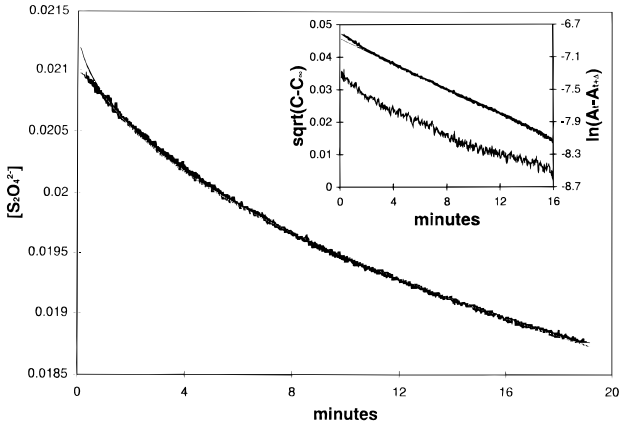

FIGURE 1: Progress curve for $S_2O_4^{2-}$ utilization. The rate of decrease of the $S_2O_4^{2-}$ concentration (molar) with time for the nitrogenase assay system at a 3.7 Av2/Av1 ratio. All components for nitrogenase activity were present in a 1.0 mL optical cell (1 cm path length), and the reaction was initiated by Av2 addition. The change in $S_2O_4^{2-}$ concentration was monitored at 375 nm ($\epsilon = 71\ M^{-1}\ cm^{-1}$) at 0.2 absorbance range and 1.4 absorbance offset. The solid line is the computed fit for a half-order reaction in $S_2O_4^{2-}$. In the inset, the upper curve is a plot of the square root of the remaining $S_2O_4^{2-}$ concentration (left vertical axis) against time. The solid line is the computed fit for a half-order reaction. The lower curve is the natural logarithm of the $S_2O_4^{2-}$ concentration (right vertical axis) against time and is clearly not linear, excluding a first-order reaction.

rejected both by inspection of Figure 1 and by fitting. A half-order reaction in $[S_2O_4^{2-}]$ gave the best fit compared to zero- or first-order reactions. The precise half-order fit is shown as the solid line in Figure 1.

The more traditional treatment of plotting $[S_2O_4^{2-}]^{1/2}$ versus time, shown in the inset of Figure 1, is linear, confirming a half-order reaction in $[S_2O_4^{2-}]$; a first-order (exponential) fit is shown for comparison and is seen to represent the data less well.

Closer inspection of the calculated fit in Figure 1 or the linearized plot in the inset shows a small departure from linearity during the first ~30 s after the Av2/Av1-catalyzed reaction was initiated. The cause of this deviation seemed to rise from a combination of temperature reequilibration, slight $S_2O_4^{2-}$ oxidation during Av2 addition, or adjustments in the absorbance of Av1 and Av2 as they reach their steady-state concentrations (see later).

Identical results [data not shown; but see Watt (1977) and Watt and Burns (1977) for application of the amperometric method] for the conditions used in Figure 1 were obtained by monitoring $[S_2O_4^{2-}]$ decrease amperometrically over a 10−20 mM $S_2O_4^{2-}$ concentration range. This method is very sensitive to changes in $[S_2O_4^{2-}]$ and unlike the optical technique is independent of the presence of bubbles, small particles, and path length, allowing measurements to be carried out more precisely over longer time intervals. Such measurements confirm the conclusion arrived at above regarding the half-order dependence on $[S_2O_4^{2-}]$ shown in Figure 1.

H_2-Evolution with Limiting $S_2O_4^{2-}$. Figure 2 shows the H_2-evolution profile obtained by manometric measurements as a function of time for an assay mixture initially containing 14 mM $S_2O_4^{2-}$. This concentration was chosen because Hageman and Burris (1978) reported that nitrogenase activity was saturated at this concentration and above. A final value of 0.95 $H_2/S_2O_4^{2-}$ was determined, providing a means to calculate the $[S_2O_4^{2-}]$ remaining at each point on the curve

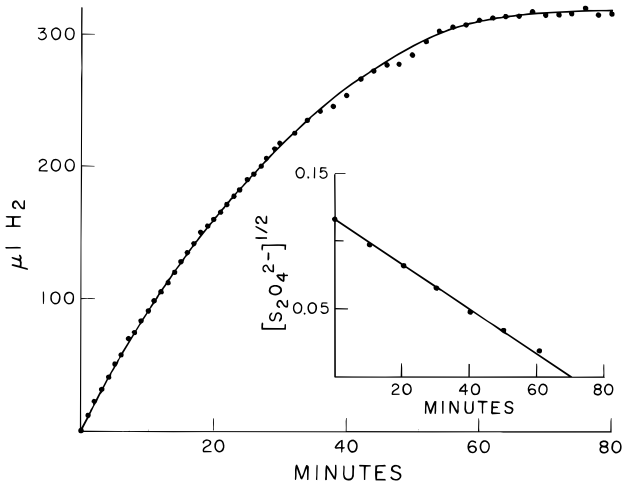

FIGURE 2: Nitrogenase-catalyzed H_2 evolution. H_2 evolved from a 1.0 mL assay contained in a Warburg manometer as a function of time at 30 °C. The initial $S_2O_4^{2-}$ concentration was 0.014 M, and the Av2/Av1 ratio was 1.75. Measurements were made every minute for the first 30 min and every 2 min thereafter. The solid line was drawn from the integrated form of eq 1. The inset is a plot of the square root of the remaining $S_2O_4^{2-}$ concentration as a function of time.

using: initial $[S_2O_4^{2-}] - H_2$ evolved = remaining $[S_2O_4^{2-}]$. The inset to Figure 2 is a plot of the square root of the remaining $[S_2O_4^{2-}]$ against time, demonstrating that the rate of H_2 evolution strictly depends on the square root of the remaining $S_2O_4^{2-}$ concentration as shown by eq 1. The

$$\frac{d[H_2]}{dt} = k[S_2O_4^{2-}]^{1/2} \quad (1)$$

integrated form of eq 1 is the mathematical function for total H_2 evolved with time from which the solid line in Figure 2 is calculated. The quality of fit is excellent, demonstrating that a strictly obeyed half-order reaction in $[S_2O_4^{2-}]$ occurs over the entire concentration range studied. An earlier report (Watt & Burns, 1977) that H_2 was evolved in a zero-order reaction is incorrect. That conclusion was made from observing the initial, near-linear portion of a curve similar to Figure 2 and concluding, like Hageman and Burris (1978), that a zero-order reaction was operative. The precise fitting of data to proposed reaction orders is a more reliable method for determining reaction orders than taking tangents to the progress curve.

The results in Figures 1 and 2, the amperometric results reported here, and previous results (Watt & Burns, 1977; Watt, 1990) all clearly demonstrate a half-order reaction in $[S_2O_4^{2-}]$ for the nitrogenase-catalyzed H_2-evolution reaction up to at least 21 mM. All of these results are *inconsistent* with those of Hageman and Burris (1978), who reported saturation with $S_2O_4^{2-}$ at 14 mM. If the results in Figure 1 were obtained under low-resolution conditions, the observed curvature would be difficult to detect, and when tangents to such a curve are drawn [as was done by Hageman and Burris (1978)], all would appear to have the same slope, suggesting saturation in $S_2O_4^{2-}$ at high concentration. The results in Figure 1 and the computer fitting of large numbers of measured data points clearly show the true half-order reaction of $S_2O_4^{2-}$ and clearly establish this kinetic feature of nitrogenase catalysis.

The K_m values for $S_2O_4^{2-}$ calculated by Hageman and Burris (1978) from perceived saturation by $S_2O_4^{2-}$ and used in their analysis of nitrogenase reactivity are, at best, much too low and are likely inappropriate. Another possible complication in the calculation of their K_m values for $S_2O_4^{2-}$ is the assumption that V_{max} for Av1 is independent of Av2 concentration. This assumption shifts any variation of K_m/V_{max} solely to variation in K_m. The validity of this assumption is considered next.

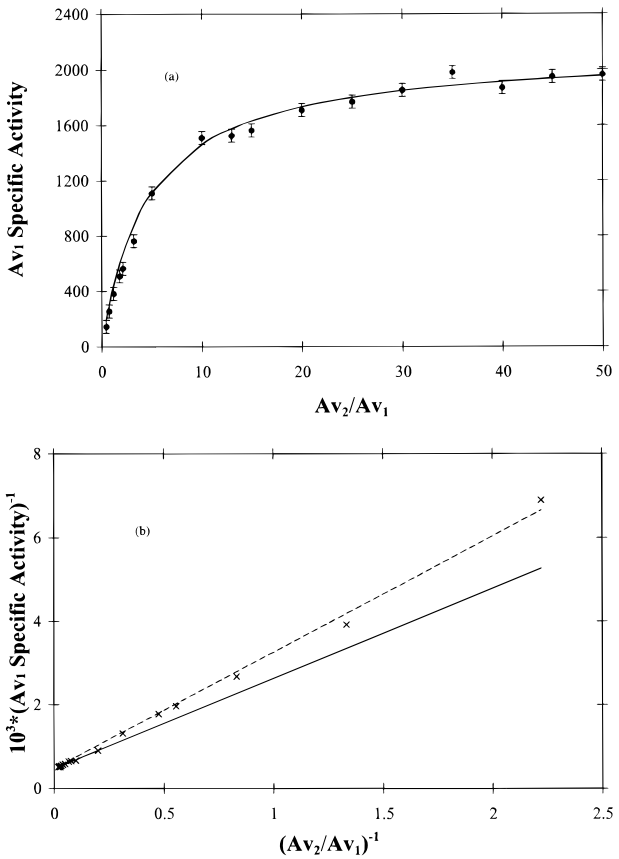

FIGURE 3: Variation of Av specific activity with Av2/Av1 ratio. (a) The specific activity of Av1 (1.71 Mo/Av1) from 10 min quenched H_2-evolution assays as a function of Av2/Av1 ratio. (b) 1/Av1 activity from (a) plotted against 1/(Av2/Av1) concentration. The Av2/Av1 ratio was varied by 125 (0.4−50) with Av2 containing 3.89 Fe atoms and Av1 containing 1.71 Mo atoms. A V_{max} value of 2134 nmol of $H_2 \cdot min^{-1} \cdot mg^{-1}$ (1.71 Mo) or 2510 nmol of $H_2 \cdot min^{-1} \cdot mg^{-1}$ (2 Mo) and K values of 4.6 μM (dashed line) and 5.9 μM (solid line) were calculated as outlined in the text.

H_2-Evolution Rate as a Function of Av2/Av1 Ratio. The rate of H_2 evolution as a function of Av2/Av1 ratio was previously analyzed (Watt, 1980; Jacobs et al., 1995) and suggested a 1:1 interaction between Av2 and Av1. Those initial studies were extended to higher Av2/Av1 ratios and higher $S_2O_4^{2-}$ concentrations in the present study using both optical and amperometric methods to gain a precise rate law for the Av2−Av1 interaction. Increasing the Av2/Av1 ratio at constant Av1 significantly increases the rate of H_2 evolution (or $S_2O_4^{2-}$ disappearance) as shown in Figure 3a; however, the half-order dependence on $[S_2O_4^{2-}]$ persists, showing that Av2 is the species which modulates the rate of electron transfer from $SO_2^{-\bullet}$ ($S_2O_4^{2-} = 2SO_2^{-\bullet}$; Crutz & Sutin, 1974) through Av1 to the product H_2.

Figure 3a appears hyperbolic and was initially analyzed by a double-reciprocal plot, giving the dashed line in Figure 3b. This line is a good fit, but there appears to be a slight upward trend in the data points corresponding to low ratios near 1 and below in Figure 3a. The *x*-axis in Figure 3a is

[total Av2]/[total Av1], and any Av2 "tied up" in a complex with Av1 during catalysis or free but otherwise unavailable (i.e., Av2ox slow to be reduced) would effectively lower the free Av2 concentration (and the Av2/Av1 ratio) and shift the points at low Av2/Av1 ratios in Figure 3a toward the *y*-axis. The reciprocal of these smaller values would increase their position on the *x*-axis in Figure 3b, consistent with the apparent upward trend. In order to evaluate this possibility, Av2/Av1 values[1] above 5 (where the steady-state assumption that Av2 > Av1 is valid) in Figure 3a were used to construct another double-reciprocal plot shown as the solid line in Figure 3b. Apparent K values from the two double-reciprocal plots are 4.6 μM (dashed line) and 5.9 μM (solid line) with identical V_{max} values of 2134 nmol·min^{-1}·(mg of Av1)$^{-1}$ obtained from Figure 3b. Assuming the upper limit K of 5.9 μM to be correct and using a V_{max} of 2134 nmol·min^{-1}·mg^{-1}, the actual concentration of free Av2 was calculated at each point in Figure 3a using eq 2. The results show that at the lowest ratio of 0.4 in Figure 3a, the concentration of free Av2 is 20−25% lower[2] than total Av2, and that the free Av2 concentration is 20−14% lower than total Av2 up to a ratio of 3.2. Above this ratio, the difference between the free and total Av2 concentrations becomes indistinguishable.

The data in Figure 3a were also fit to a rectangular hyperbola using the Applied Photophysics Kinetics Global Analysis Program employing the Marquardt algorithm in an iterative cycle which calculated the best fit for free Av2 from total Av2. The results gave V_{max} and K values of 2150 ± 60 nmol·min^{-1}·mg^{-1} and 5.3 ± 0.5 μM, respectively, in agreement with the above analysis.

The inherent experimental uncertainty in the data in Figure 3a is estimated to be 7−9%; therefore, the corrected data in Figure 3a, represented by the solid line in Figure 3a, are small but appear significant. The rate law for H_2 evolution and acetylene reduction is completely specified at a given $S_2O_4^{2-}$ concentration and at constant MgATP concentration of 5 mM by eq 2, where V_{max} is 2510 nmol of H_2·min^{-1}·mg^{-1} (a V_{max} of 2134 nmol·min^{-1}·mg^{-1} from Figure 3a normalized from 1.7 to 2.0 Mo/Av1), K is 5.9 μM, and [Av2] is the concentration of free Av2.

$$v = \frac{d[H_2]}{dt} = \frac{k_{cat}[Av1][Av2]}{K + [Av2]} = \frac{V_{max}[Av2]}{K + [Av2]} \qquad (2)$$

In addition to establishing the precise rate law for the Av1−Av2 interaction, eq 2 and the above analysis provide a basis for also understanding the concentration of oxidized Av2 observed in the steady state. Below we will present evidence that during catalytic turnover up to 25% of Av2 is in the Av2ox form, perhaps accounting for the "unavailable" Av2 noted in Figure 3.

Av2−Av1 Steady State. EPR studies of the Av (Orme-Johnson et al., 1972), Cp (Mortenson et al., 1973), and Kp (Smith et al., 1973) nitrogenase systems demonstrated that the MoFe protein components (Av1, Cp1, and Kp1, respectively) were nearly EPR-silent (and presumably "super reduced") while the EPR intensity of the Fe protein components (Av2, Cp2, and Kp2 respectively) decreased,

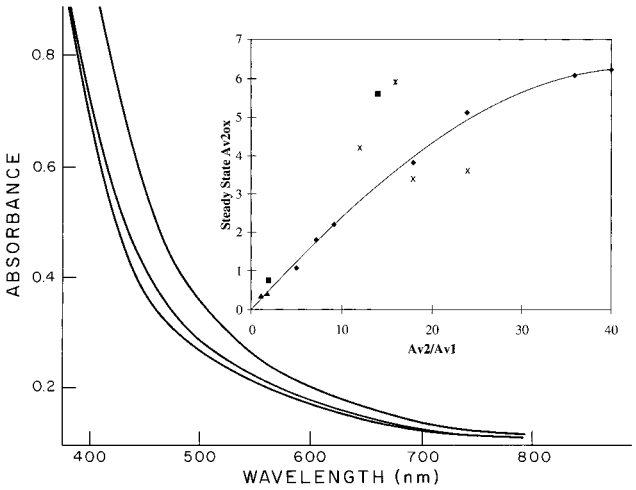

FIGURE 4: Optical measurements of Av2ox during steady-state turnover. The standard nitrogenase assay (minus ATP) containing 2.9 μM Av1 and 70.5 μM Av2 (Av2/Av1 = 24) in 5 mM $S_2O_4^{2-}$ contained in a 1.0 mL quartz cell (bottom spectrum). After addition of 50 μL of 0.1 M ATP, the nitrogenase system reached steady state, and the middle spectrum was recorded after 2 min. After all $S_2O_4^{2-}$ was consumed, the oxidized Av2 spectrum was recorded (top spectrum). The inset contains the number of Av2ox per Av1 determined by optical and EPR spectroscopy in the steady state as a function of the Av2/Av1 ratio. The more extensive optical data (♦) are connected by a line to aid comparison. The EPR data are from this study (×) and Mortenson et al. (1973) (■), Smith et al. (1973) (▲), and Orme-Johnson et al. (1972) (∗).

presumably due to formation of oxidized Fe protein. These qualitative results can be quantitated using the reported steady-state Fe protein EPR signal heights (and appropriate controls) to show that at Fe/MoFe ratios of 1 (0.36), 1.67 (0.42), 1.82 (0.76), 14 (5.6), and 16 (5.9), the number of oxidized Fe proteins per MoFe protein, shown in parentheses, are formed at steady state. These results show two effects: (1) a significant number of oxidized Fe proteins are present per MoFe protein in the steady state; and (2) the total amount formed increases with ratio. Using Av2/Av1 ratios of 12, 18, and 24 at steady state, integrating their signal-averaged spectra, and comparing them to appropriate controls, our results indicate that the Av2red concentration has decreased 35%, 19%, and 15% during steady state, corresponding to the presence of 4.2, 3.4, and 3.6 Av2ox, respectively. The above EPR integration results were measured only over the $g = 2$ region even though the iron protein is known to have an $S = {}^3/_2$ component in the $g = 4$ region. Extensive EPR and Mossbauer studies (Lindahl et al., 1985; Hagen et al., 1985; Watt & McDonald, 1985) of Av2 under various conditions have shown that the amounts of these two spin states remain constant under a variety of conditions. Lindahl et al. (1985) found similar spin-state mixtures even for Av2 under steady-state turnover conditions. These published results argue that the low EPR integration is not due to conversion of $S = {}^1/_2$ to $S = {}^3/_2$ during steady state and that the integrated intensity (or previous signal height results) is a result of conversion of reduced Av2 into oxidized Av2 (Orme-Johnson et al., 1972). These EPR results are consistent with optical measurements of Av2ox in the steady state discussed next.

Figure 4 shows the optical spectrum (bottom) of reduced Av2 and Av1 with excess $S_2O_4^{2-}$ at a 24:1 ratio before MgATP is added to produce the middle, steady-state spectrum. When all $S_2O_4^{2-}$ was consumed, the upper spectrum was recorded which corresponds to complete

[1] Initially the calculation was made at an Av2/Av1 ratio of 10 where the approximation Av2 > Av1 would be totally valid, but no significant difference was found if the value of 5 or even 3.2 was used.

[2] The actual percentages could be slightly lower since they are based on the upper limit value of 5.9 μM for K in eq 2.

oxidation of Av2red to Av2ox, presumably as either Av2ox-$(MgATP)_2$ or Av2ox$(MgADP)_2$. This conclusion is supported by (1) adding $S_2O_4^{2-}$ and reproducing the middle spectrum and (2) coulometrically reducing samples removed from the optical cell after dithionite depletion and showing that 1.1 ± 0.2 electrons are transferred per Av2 present. If the coulometrically measured level of oxidation was attributed to Av1, this would require Av1 to be oxidized by the unrealistically high value of 24 electrons. Furthermore, the enzymatic oxidation of Av2 by Av1 as followed by both EPR and optical measurements as dithionite is depleted demonstrated (Larsen et al., 1995) that the optical and EPR properties are closely correlated and correspond to Av2 oxidation and not to Av1 oxidation. From these results, we conclude that the middle spectrum of Figure 4 is due to Av2ox present during the steady state. Av2ox is likely to be in its ATP or ADP form, but because the exact state remains unknown, we use Av2ox to designate oxidized Av2 in the steady state.

The fraction of Av2ox present in Figure 4 is calculated by dividing the optical change at steady state (middle spectrum) by that for complete conversion to Av2ox (upper spectrum). The solid line in the inset to Figure 4 describes how the steady-state level of Av2ox changes as a function of the Av2/Av1 ratio. At low ratios, corresponding to a low Av1 turnover rate, Av2ox is at relatively low levels, but as the ratio increases, its concentration relative to Av1 increases until it finally levels off near 6 at high ratios.

The observed Av2ox intermediate is surprisingly unreactive. For example, at a ratio of 18 corresponding to 3.8 Av2ox and 14.2 Av2red per Av1, respectively, Av2ox remained oxidized in the presence of 5−10 mM dithionite present in the assay mixture. In addition, separate experiments showed it remained oxidized with a 2-fold increase in both [MgATP] and [$S_2O_4^2$]. This lack of response of Av2ox toward $S_2O_4^{2-}$ reduction at this ratio and others indicates that Av2ox present during steady state either is (1) physically incapable of reacting with $S_2O_4^{2-}$ (in a tight complex with Av1 which must dissociate prior to reaction with $S_2O_4^{2-}$) or (2) in a free but conformationally modified or ligand-altered unreactive state [i.e., Av2ox$(MgADP)_2$]. Possibility (1) requires the unlikely condition that at a ratio of 18, 3.8 Av2ox are bound to each Av1, and more than 6 are bound at even higher ratios. This possibility seems unlikely. If possibility (2) is correct, then the rate of reduction of Av2ox [possibly in the Av2ox$(MgADP)_2$ form] to Av2red occurs at a comparable rate to nitrogenase turnover. Although direct measurements for reduction of Av2ox have not been reported, the reductive conversion of Kp2ox$(ADP)_2$ into Kp2red$(ADP)_2$ (Thorneley & Lowe, 1983; Ashby & Thorneley, 1987) occurs just faster than nitrogenase turnover and supports this conclusion.

The steady-state optical and EPR results obtained in this study and previously published EPR results discussed above are compared in the inset of Figure 4. The initial slope of the line up to a ratio of 10−12 is about 0.25, corresponding to 25% of Av2 being in the Av2ox form. Analysis of Figure 3 using eq 2 demonstrated that up to 25% of the total Av2 was unavailable for interaction with Av1 during steady-state kinetic measurements. The 25% of total Av2 in the free Av2ox form observed under steady-state conditions may account for the missing Av2 in Figure 3. The present results indicate that all the Av2ox is accounted for and, therefore, do not support the view that the rate-limiting step for Av nitrogenase is dissociation of the Av1−Av2 redox complex, in which significant Av2ox should be bound.

Taken together, the steady-state kinetic results show that (1) the Av2ox intermediate is formed as a consequence of interaction with Av1, (2) up to 25% of total Av2 exists as free Av2ox at steady state, (3) Av2ox is quite unreactive toward dithionite, and (4) its formation (inset to Figure 4) is similar to that shown in Figure 3a.

DISCUSSION

High-precision kinetic measurements and analysis have been carried out which address three areas of *Azotobacter vinelandii* nitrogenase catalysis: (1) the reaction order of $S_2O_4^{2-}$ under optimal kinetic conditions; (2) the kinetic relationship between Av2 and Av1 during catalysis; and (3) the formation of the Av2ox intermediate under steady-state conditions. Each of these topics is relevant to understanding the complex reactions occurring during nitrogenase catalysis, and high-precision measurements and analysis have been conducted to clearly establish their kinetic relationships.

Reaction Order of $S_2O_4^{2-}$. The point where electrons (reductant) enter the sequence of reactions occurring during nitrogenase catalysis has been examined (Watt, 1977; Watt & Burns, 1977; Hageman & Burris, 1978). Watt and Burns (1978) concluded that reductant entered after ATP was bound because $S_2O_4^{2-}$ saturation was not observed. However, the validity of this conclusion and the half-order $S_2O_4^{2-}$ dependence initially observed were questioned when Hageman and Burris (1978) reported an apparent zero-order reaction in $S_2O_4^{2-}$ and concluded that saturation by $S_2O_4^{2-}$ did occur. Furthermore, from their kinetic measurements which suggested saturation by dithionite, K_m values for $S_2O_4^{2-}$ were determined which varied with conditions such as $S_2O_4^{2-}$ concentration, nitrogenase protein ratios, and the presence of flavoprotein. These variations in K_m values were interpreted mechanistically, and conclusions were drawn (Hageman & Burris, 1978) that form some of the presently accepted concepts of nitrogenase function. However, if saturation does not occur, then the calculated K_m values are not valid. The disagreement in the reaction order in $S_2O_4^{2-}$ (half vs zero) clearly has important implications in understanding nitrogenase function. To resolve this uncertainty, it is only necessary to establish definitively whether $S_2O_4^{2-}$ is a saturating (zero-order) or nonsaturating (half-order) substrate at $S_2O_4^{2-}$ concentrations >14 mM.

The kinetic curve for $S_2O_4^{2-}$ utilization shown in Figure 1 at 21 mM was obtained using the same method originally used by Hageman and Burris (1978) and is clearly not linear. This result immediately excludes a zero-order (saturating) reaction in $S_2O_4^{2-}$ and requires a higher reaction order. Kinetic analysis of Figure 1 is definitive in showing that the reaction is half-order in [$S_2O_4^{2-}$] up to 21 mM. This result was confirmed by the amperometric method which is more sensitive than the optical one and has fewer complexities. In addition, a calorimetric method was developed (Watt, 1990) which uniquely gives the reaction order by inspection of the shape of the thermogram (heat liberated *versus* time) which unequivocally excludes a zero-order reaction and confirms the half-order reaction for $S_2O_4^{2-}$. Finally, Figure 2 demonstrates that the rate of H_2 evolution follows a strictly obeyed half-order reaction until all $S_2O_4^{2-}$ is consumed. H_2 evolution was the measured quantity, but because H_2 evolved and $S_2O_4^{2-}$ consumed are stoichiometrically linked, the H_2

evolution rate mirrors the rate law for $S_2O_4^{2-}$ decrease. The result of Figure 2, therefore, also confirms the half-order rate law in $S_2O_4^{2-}$ at high $S_2O_4^{2-}$ concentration.

The lack of saturation by $S_2O_4^{2-}$ at experimentally accessible concentrations can be understood in more fundamental terms by considering the chemical behavior of $S_2O_4^{2-}$. The half-order reaction arises from $SO_2^{-\bullet}$, derived from $S_2O_4^{2-}$ dissociation ($S_2O_4^{2-} = 2SO_2^{-\bullet}$, $K_{diss} = 1.4 \times 10^{-9}$ M), being the actual reductant for the nitrogenase-catalyzed H_2-evolution reaction. At 20 mM $S_2O_4^{2-}$, the $SO_2^{-\bullet}$ concentration is calculated to be 5.3 μM, a value near Av2 concentrations of 2.5−10 μM typically used during nitrogenase assays. Under steady-state conditions, the concentration of $SO_2^{-\bullet}$ would be even lower, creating conditions where $SO_2^{-\bullet}$ could not possibly be saturating; therefore, the half reaction order shown in Figure 1 is to be expected. Eventual saturation by $SO_2^{-\bullet}$ is not practical even at higher $S_2O_4^{2-}$ concentrations because its concentration rises only with the square root of the [$S_2O_4^{2-}$], and Table 1 shows that [$S_2O_4^{2-}$] concentrations higher than 20 mM become inhibitory.

Av2/Av1 Ratio. The improper calculation of K_m values for $S_2O_4^{2-}$ reported by Hageman and Burris (1978) is even more problematic when considering perceived K_m variation with increasing Av2/Av1 ratios. Variation of K_m/V_{max} at selected Av2/Av1 ratios was attributed solely to K_m variation because it was assumed that V_{max} for Av1 was invariant with increasing Av2 levels. Figure 3 shows that this assumption is not valid. Thus, the reported variation of K_m/V_{max} with Av2 was improperly attributed to the variation of K_m for $S_2O_4^{2-}$ instead of the actual variation in V_{max} shown in Figure 3.

The nitrogenase activity shown in Figure 3 is described by a well-defined rate law given by eq 2 which precisely relates the interaction between Av1 and Av2 at ratios above 0.4. This 1:1 relationship holds for a 125-fold variation of the Av2/Av1 ratio and represents Av2 transferring a single electron to Av1 during nitrogenase catalysis. From 0.4 to about 15, the activituy of Av1 increases significantly with Av2/Av1 ratio but then begins to level off, indicating that Av1 becomes saturated with Av2. When saturated, electron transfer from Av2 to Av1 is maximized, and the rate-limiting step shifts to a different kinetic event. The Thorneley and Lowe (1985) model would suggest that the separation of Av2ox from Av1 is the rate-limiting step; however, at present, the results reported here are not fully in accord with this interpretation.

The Av2ox Intermediate. EPR and optical spectroscopy are consistent in showing (Figure 4) that Av2ox represents up to 25% of total Av2 during steady-state enzyme turnover. This result implies that conversion of Av2ox to Av2red is a relatively slow step, a result consistent with the hypothesis integrated into the Thorneley and Lowe scheme that dissociation of Av2ox from a 1:1 complex with Av1 would be the rate-limiting step in Av nitrogenase catalysis. However, at ratios above about 5, both EPR and optical measurements show that more than 1 Av2ox is formed per Av1 and that values greater than 6 are observed at higher ratios. These results are inconsistent with the presence of a single Av2ox dissociating from a 1:1 complex as proposed in the Thorneley and Lowe scheme and indicate that free Av2ox is present which is slow to react with excess dithionite. The buildup of the Av2ox intermediate must be a consequence of a slow reaction converting free Av2ox back into Av2red and not just its dissociation from the complex. Explaining the EPR results and the results in Figures 3 and 4 in terms of the Thorneley and Lowe scheme for the Av nitrogenase system is not straightforward, and further evaluation is underway.

REFERENCES

Ashby, G. A., & Thorneley, R. N. F. (1987) *Biochem. J. 246*, 455.

Bulen, W. A., Burns, R. C., & Le Comte, J. R. (1965) *Proc. Natl. Acad. Sci. U.S.A. 53*, 532.

Burgess, B. K., Jacobs, D. B., & Stiefel, E. I. (1980) *Biochim. Biophys. Acta 614*, 196.

Burns, A., Watt, G. D., & Wang, Z.-C. (1985) *Biochemistry 24*, 3932.

Crutz, C., & Sutin, N. (1974) *Inorg. Chem. 13*, 2041−2043.

Deits, T. L., & Howard, J. B. (1990) *J. Biol. Chem. 265*, 3859.

Hageman, R. V., & Burris, R. H. (1978) *Biochemistry 17*, 4117.

Hageman, R. V., Orme-Johnson, W. H., & Burris, R. H. (1980) *Biochemistry 19*, 2333.

Hagen, W. R., Eady, R. R., Dunham, W. R., & Haaker, H. (1985) *FEBS Lett. 189*, 250.

Jacobs, D., Mitchell, D., & Watt, G. D. (1995) *Arch. Biochem. Biophys. 324*, 317.

Kim, J., & Rees, D. C. (1994) *Biochemistry 33*, 389.

Larsen, C., Christensen, S., & Watt, G. D. (1995) *Arch. Biochem. Biophys. 323*, 215.

Lindahl, P. A., Gorelick, N. J., Munck, E., & Orme-Johnson, W. H. (1985) *J. Biol. Chem. 262*, 14945.

Ljones, T. (1973) *Biochim. Biophys. Acta 321*, 103.

McKenna, C., Gutheil, W. G., & Song, W. (1991) *Biochim. Biophys. Acta 1075*, 109.

Mortenson, L. E., & Thorneley, R. N. F. (1979) *Annu. Rev. Biochem. 48*, 387.

Mortenson, L. E., Zumft, W. G., & Palmer, G. (1973) *Biochim. Biophys. Acta 292*, 422.

Noguchi, T. (1971) *Chem. Abstr. 74*, 33174.

Orme-Johnson, W. H. (1985) *Annu. Rev. Biophys., Biophys. Chem. 14*, 419.

Orme-Johnson, W. H., Hamilton, W. D., Ljones, T., Tso, M.-Y., Burris, R. H., Shah, V. K., & Brill, W. J. (1972) *Proc. Natl. Acad. Sci. U.S.A. 69*, 3142.

Silverstein, R., & Bulen, W. A. (1970) *Biochemistry 9*, 3809.

Smith, B. E., & Eady, R. R. (1992) *Eur. J. Biochem. 205*, 1.

Smith, B. E., Lowe, D. J., & Bray, R. C. (1973) *Biochem. J. 135*, 331.

Stephens, P. J., McKenna, C. E., McKenna, M.-C., Nguyen, H. T., & Lowe, D. J. (1983) in *Electron Transport and Oxygen Utilization* (Ho, C., Ed.) pp 405−409, Macmillan, New York.

Thorneley, R. N. F., & Eady, R. R. (1973) *Biochem. J. 133*, 405.

Thorneley, R. N. F., & Lowe, D. J. (1983) *Biochem. J. 215*, 393.

Thorneley, R. N. F., & Lowe, D. J. (1984a) *Biochem. J. 224*, 887.

Thorneley, R. N. F., & Lowe, D. J. (1984b) *Biochem. J. 224*, 903.

Thorneley, R. N. F., & Lowe, D. J. (1985) in *Molybdoenzymes* (Spiro, T. G., Ed.) p 221, John Wiley & Sons, New York.

Watt, G. D. (1977) in *Recent Developments in Nitrogen Fixation* (Newton, W. E., Postgate, J. R., & Rodriguez-Barrueco, C., Eds.) p 179, Academic Press, London.

Watt, G. D. (1979) *Anal. Biochem. 99*, 399.

Watt, G. D. (1980) in *Molybdenum Chemistry of Biological Significance* (Newton, W. E., & Otsuka, S., Eds.) p 3, Plenum Press, New York & London.

Watt, G. D. (1990) *Anal. Biochem. 187*, 141.

Watt, G. D., & Bulen, W. A. (1974) in *Nitrogen Fixation* (Newton, W. E., & Nyman, C. J., Eds.) p 248, Washington State University Press, Pullman, WA.

Watt, G. D., & Burns, A. (1977) *Biochemistry 16*, 264.

Watt, G. D., & McDonald, J. W. (1985) *Biochemistry 24*, 7226.

Watt, G. D., Bulen, W. A., Burns, A., & Hadfield, L. K. (1975) *Biochemistry 14*, 4266.

Watt, G. D., Wang, Z.-C., & Knotts, R. R. (1986) *Biochemistry 25*, 8156.

Wherland, S., Burgess, B. K., Stiefel, E. I., & Newton, W. E. (1981) *Biochemistry 20*, 5132.

Yates, M. G., Thorneley, R. N. F., & Lowe, D. J. (1975) *FEBS Lett. 60*, 89.

BI952581O